

*Environmental Toxicology*BIOACCESSIBLE HEAVY METALS-SEDIMENT PARTICLES FROM RECONQUISTA RIVER  
INDUCE LUNG INFLAMMATION IN MICESEBASTIÁN A. FERRARO,<sup>†‡</sup> GUSTAVO CURUTCHET,<sup>†§</sup> and DEBORAH R. TASAT\*<sup>†||</sup><sup>†</sup>Center of Studies in Health and Environment, School of Science and Technology, National University of General San Martín, San Martín, Buenos Aires, Argentina<sup>‡</sup>Committee for Scientific Research, Buenos Aires, Argentina<sup>§</sup>Center of Environmental Studies 3iA, National University of General San Martín, San Martín, Buenos Aires, Argentina<sup>||</sup>Department of Histology and Embryology, School of Dentistry, University of Buenos Aires, Buenos Aires, Argentina

(Submitted 17 January 2012; Returned for Revision 1 May 2012; Accepted 10 May 2012)

**Abstract**—The Reconquista River (RR), one of the most polluted watercourses in Argentina, receives effluent discharges from heavily industrialized and highly populated settlements. During winter and summer, the floodplain remains dry, producing the oxidation of sulfide and organic matter present in the sediment, making heavy metals more bioaccessible. Dispersion of this sediment occurs, and thus harmful effects on the pulmonary health of residents and workers inhabiting the RR bank may take place. The authors characterized the sediment particles of the RR (RR-PM) morphologically by scanning electron microscopy and its elemental composition by energy dispersive X-ray spectroscopy (EDX) and Community Bureau of Reference (BCR) sequential extraction. Furthermore, the authors evaluated its biological impact on the respiratory system of BALB/c mice, generating four groups: control healthy, sensitized with ovalbumin, exposed to particles, and sensitized and exposed to particles. Sediment particles of the Reconquista River contained fine particulate matter, with a high concentration of bioaccessible Cu and Zn. The authors found that animal exposure to RR-PM caused polymorphonuclear cell lung infiltration, augmentation of O<sub>2</sub><sup>-</sup>, increase of proinflammatory cytokines (tumor necrosis factor alpha [TNF $\alpha$ ], interleukin-6 [IL-6]) and apoptosis. This adverse response was more dramatic in the sensitized and exposed to particles group. Even more, they proved the bioaccessible fraction present in the RR-PM to be responsible for these harmful effects. The authors conclude that RR-PM produces an adverse biological impact on the airways of healthy animals, which is largely aggravated in previously sensitized animals. Environ. Toxicol. Chem. © 2012 SETAC

**Keywords**—Reconquista River    Sediment toxicity    Particulate matter    Heavy metals    Lung

## INTRODUCTION

The Reconquista River (RR) Basin is located in the northern metropolitan area of Buenos Aires, Argentina. The RR has an extension of 1,547 km<sup>2</sup> receiving effluent discharges from heavily industrialized and highly populated settlements; thus, at present, no site of the river can be characterized as being free of pollutants. It runs through 18 districts of the metropolitan area of Buenos Aires, supporting more than four million inhabitants. The activity of a wide range of industries (textile, mills, chemicals, slaughterhouses, and so forth) in the district of General San Martín—the second largest industry area in the metropolitan area of Buenos Aires—generates enormous volumes of solid, liquid, and gaseous waste that has to be subject to appropriate management to minimize environmental impact [1–3]. According to the American Health Organization, less than 10% of the municipalities in Latin America treat sewage adequately before emptying it into natural watercourses; furthermore, both wastewater treatment plants and sewers for industrial effluents are often not working or are nonexistent [4]. When waste treatment or waste disposals are unsuitable, the environmental impact is large, affecting not only the air, water, and soil, but also the health of its residents.

In the San Martín district, many of the effluents and residues are discharged to the RR, turning it into a peri-urban, highly

polluted river and converting it into a landmark of Buenos Aires with serious environmental problems. In 2006, Castañé et al. [5] analyzed an array of physicochemical parameters in the water of the RR. The study revealed significant differences in the degree of deterioration between sites along its course. These authors, in agreement with Herkovits et al. [6], have identified the Moron stream—a tributary that flows into the main course of the RR located at the grounds of San Martín district—as the worst water quality site, attributed to the discharges of a complex mixture of nontreated waste. Previous studies on the RR [6,7] provided general baseline information and attempted to explain the possible effects of industrial discharges on the aquatic environment. Essential and heavy metals are natural constituents of waters, being present at low concentrations. Nonetheless, rapid expansion of human activity has continuously accelerated the risk of environmental pollution with heavy metals. Heavy metals from both natural and anthropogenic sources are distributed between bed sediments and aqueous phases of the RR watercourse [8]. Among the various pollutants, heavy metals are the most toxic, persistent, and abundant, being able to increase their concentration through biomagnification in aquatic habitats [9–11]. Most metals are retained by the particle surfaces and are preferentially transported, deposited, and eventually buried with fine-grained sediments [12].

During winter and summer (low-water seasons), the floodplain remains dry; thus, the strongly polluted sediment may disperse into the air. Even more, particle sediment that is normally under anaerobic conditions will now be exposed at the surface, dealing with an aerobic environment. Under this new aerobic condition, oxidation of both sulfides and organic

All Supplemental Data may be found in the online version of this article.

\* To whom correspondence may be addressed

(deborah.tasat@unsam.edu.ar).

Published online 15 June 2012 in Wiley Online Library  
(wileyonlinelibrary.com).

matter present in the sediment quickly occurs as the result of the activity of the autotrophic sulfur-oxidizing bacteria and heterotrophic aerobes. This oxidation noticeably increases the bioavailability of heavy metals [13–15].

As mentioned, particles present in the RR plain sediments dry off, polluting the atmosphere. These air-suspended particles may enter the body, mainly through the respiratory tract, which in turn may elicit harmful effects on the pulmonary health of residents and workers inhabiting the RR bank. Although air particulate matter (PM) has been associated with an increase in the rates of mortality and morbidity in the population [16–18], the effect of aerosolized dust created from the RR sediments on pulmonary function remains unknown.

The purpose of the present study was primarily to characterize chemically and morphologically the particulate matter from the Reconquista River (RR-PM) at the Moron stream site and secondly to perform a preliminary assessment of the short-term exposure to inhaled RR-PM on pulmonary function on healthy and sensitized mice.

## MATERIALS AND METHODS

### *Drugs and chemicals*

Nitroblue tetrazolium (NBT), 12-O-tetradecanoylphorbol 13-acetate (TPA), ethylenediaminetetra-acetic acid (EDTA), phosphate-buffered saline (PBS), RPMI-1640 medium, polyvinylpyrrolidone, Hoechst 33258, paraformaldehyde, ovalbumin (OVA) (grade III), aluminum hydroxide, and all histological dyes employed were purchased from Sigma-Aldrich. Purified monoclonal antibodies for interleukin-6 (IL-6) and tumor necrosis factor alpha (TNF $\alpha$ ) were purchased from BD Pharmingen; anti-poly-adenosine diphosphate ribose polymerase p85 fragment polyclonal antibody (pAB) and anti-active caspase-3 pAB were purchased from Promega. Horseradish peroxidase–streptavidin conjugate was obtained from Zymed Laboratories, 3,3',5,5'-tetrametilbenzidin from Dako Cytomation, and VECTASTAIN Elite ABC Kit, PK-6200 from Vector Laboratories.

### *Animals*

Male BALB/c mice two to three months of age were obtained from the animal facilities of the School of Exact and Natural Sciences of the University of Buenos Aires and housed according to the National Institutes of Health Guide for the Care and Use of Laboratory Animals and to the ad hoc committee of the National University of General San Martín at the breeding facility of the School of Science and Technology, University of San Martín, for use throughout these experiments. Animals were fed a normal protein diet and water ad libitum. All experiments complied with local ethical guidelines.

### *Particle sampling and analysis*

Superficial composite samples of the dry sediment were taken with a shovel (0–5 cm). Samples collected during winter in the dry zone of the basin adjacent to the course of the river where it meets the Morón tributary were placed in plastic containers and stored at 4°C. Before any experiment was carried out, the RR samples were chemically characterized.

Scanning electron microscopy (SEM) and energy dispersive X-ray spectroscopy (EDX) were employed to analyze particle morphology and chemical composition. For SEM observations, collected particles were coated with silver by direct current sputtering. Stub preparations were examined in a Philips 515 SEM (Philips Electron Optics, NL) and EDX 4100 with a silicon–lithium detector.

### *Extraction and quantification of heavy metals from RR-PM*

Metals were extracted from dry RR-PMs following a metal sequential extraction procedure (Community Bureau of Reference [BCR] protocol) [19] standardized by the U.S. Environmental Protection Agency (U.S. EPA). Heavy metals' pseudo-total content was determined by boiling 0.5 g sediment with aqua regia (30 ml) for 1 h, allowing them to cool, and then filtering through blue ribbon paper filter. Digests were diluted to 50 ml with distilled water, and metal content was analyzed using flame atomic absorption spectrometry. A bioaccessible fraction of metals was studied by extraction with 0.1 M EDTA (pH = 5.5) overnight followed by flame atomic absorption spectrometry [20]. The four sequential extraction steps used 0.11 mol/L acetic acid (step 1: exchangeable and water–acid-soluble like carbonate-bound metals); 0.1 mol/L hydroxylammonium chloride acidified with HNO<sub>3</sub> (pH = 2) (step 2: Fe and Mn oxides); 8.8 mol/L hydrogen peroxide (step 3: organic matter and sulfide-bound metals); and aqua regia (step 4: residual fraction, nonsilicate-bound metals). In brief, bioaccessible metals were obtained in the first two extractions, whereas metals from the third and fourth extraction correspond to non-bioaccessible metals [21]. To avoid the harmful effect of the acetic acid or hydroxylamine chloride solutions on cells, 0.1 M EDTA was used to extract the bioaccessible fraction for ex vivo experiments [22]. Bioaccessible metal fraction extracted by this method was similar to that obtained with the first two fractions of the BCR (M.P. Di Nanno, 2009, Master's thesis, University of Buenos Aires, Buenos Aires, Argentina).

### *Sensibilization protocol*

To study the impact of particulate matter in a population with preexisting lung disease, we used a mouse model that mimics pulmonary allergy [23,24]. Sensibilization was achieved by two intraperitoneal injections of 0.2 ml PBS containing chicken OVA (grade III; Sigma-Aldrich) (100  $\mu$ g/ml) and aluminum (10 mg/ml) twice per week. One week later, mice were exposed to aerosolized OVA 3% w/v in PBS, for 10 min on three consecutive days. Aerosol exposure was performed within individual compartments in a mouse pie chamber using a nebulizer (San-Up; OVA solution flux 0–33 ml/min in air flux of 6–8 L/min).

### *Animal exposure to RR-PM*

Young BALB/c mice were exposed to RR-PM particles by intranasal instillation [25]. This technique is suitable for toxicity studies in which the pattern and uniformity of particle deposition is of primary concern [26]. For the short-term exposure treatment, particles were suspended in PBS (pH 7.2–7.4) and sonicated during 10 min before use. Animals were exposed to PM, as previously described by our group [27]. Mice were anesthetized intraperitoneally with 1 ml/kg body weight of xylazine (2%) and ketamine (50 mg/ml), and intranasally instilled with 50 ml RR-PM suspension (0.17 mg/kg body wt) three times per day, 3 d per week. Animals were killed 1 h after the last exposure with an overdose of xylazine–ketamine.

### *In vivo experimental protocol*

Animals were divided into four groups (Fig. 1): control healthy, sensitized with ovalbumin, exposed to particles, and sensitized and exposed to particles.

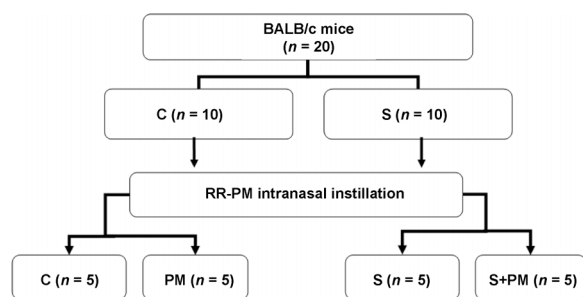


Fig. 1. In vivo experimental protocol diagram. Animals were divided into four groups: control healthy (C), sensitized with ovalbumin (S), exposed to particles (PM), sensitized and exposed to particles (S + PM).

#### Ex vivo experimental protocol

To identify whether “bioaccessible” metals present in the RR-PM are mainly responsible for superoxide anion ( $O_2^-$ ) generation or cell death by apoptosis, we evaluated the effect of the following: (1) RR-PM; (2) RR-PM treated with EDTA (0.1 M, pH = 5); (3) soluble metal fraction (SMF; “bio-accessible”); (4) RPMI-1640; and (5) EDTA (0.1 M, pH = 5) on bronchoalveolar lavage (BAL) cells from control mice. In all trials,  $0.35 \times 10^6$  cells/ml RPMI-1640 was used. Cells were incubated under constant agitation for 1 h at 37°C.

#### Bronchoalveolar lavage

Bronchoalveolar lavage was performed as previously described [28]. Briefly, the thoracic cavity was partly dissected and the trachea was cannulated with an 18-gauge needle. The excised lung was then gently massaged and lavaged 12 times with 1 ml cold, sterile, PBS ( $Ca^{++}$  Mg free, pH 7.2–7.4). The BAL fluid was immediately centrifuged at 800 g for 10 min at 4°C, and total cell number was determined with a Neubauer chamber. Based on morphological criteria, control animals showed greater than 95% of alveolar macrophages (AM). In all ex vivo experiments, a density of  $0.35 \times 10^6$  cells/ml was maintained per tube as well.

#### Total cell number and differential cell count

Total cell number (TCN) was determined with a Neubauer chamber. Bronchoalveolar lavage differential cell count was performed by fixing the cells in methanol and staining them with hematoxylin-eosin. At least 200 cells in each sample were counted by light microscopy.

#### Lung histology

Lungs from control and particle-exposed mice were excised and fixed by immersion in 10% buffered formalin, dehydrated in graded concentrations of alcohol, and routine processed for paraffin embedding and staining with hematoxylin-eosin. Histological sections of 7  $\mu$ m were cut with a Reichert-Jung micrometer (Nossloch) for optical microscopy. A morphometric analysis was performed using Image Pro Plus software (Media Cybernetics). Microphotographs of paraffin sections stained with hematoxylin-eosin from control and RR-PM-exposed mice were employed. The alveolar space area relative to the total alveolar area of the lung tissue was determined. Results were expressed as the percentage of the lumen area.

#### Generation of superoxide anion

Superoxide anion ( $O_2^-$ )—a main reactive oxygen species (ROS) generated during the respiratory burst—was evaluated

using the NBT reduction test [29] both in vivo (see experimental diagram design, Fig. 1) and ex vivo on control and particle-treated BAL cells. Superoxide anion is originated from the reduction of  $O_2^-$  by nicotinamide adenine dinucleotide phosphate-oxidase, which is localized on the surface of the plasma membrane, during the respiratory burst. The intracellular release of this ROS is evidenced by the amount of a blue formazan precipitate in the cells after NBT reduction. Bronchoalveolar lavage cells were treated with NBT in the presence or absence of TPA, a known inductor of  $O_2^-$  generation. All tubes were incubated with NBT for 60 min at 37°C. In positive controls, TPA was added at a concentration of 0.5  $\mu$ g/ml for the last 15 min. Cells were scored by light microscopy as described elsewhere [30].

#### Detection of proinflammatory cytokines (TNF $\alpha$ and IL-6)

The production of the cytokine TNF $\alpha$  was evaluated on the first supernatant of BAL fluid, and IL-6 was determined on sera from all four experimental groups. Supernatants and sera were frozen at  $-20^\circ\text{C}$  until use.

The TNF $\alpha$  and IL-6 cytokines were detected using a specific enzyme-linked immunosorbent assay. Enzyme-linked immunosorbent assay plates (Corning) were coated with 1:125 TNF $\alpha$  or 1:83 IL-6 specific capture antibody diluted in coating buffer (0.1 M sodium carbonate, pH = 6 for TNF $\alpha$ , or 0.1 M sodium phosphate, pH = 9.5 for IL-6) at 4°C overnight. Wells were washed (0.05% Tween 20) and blocked with PBS containing 10% fetal calf serum for 2 h at room temperature. Cytokine standards and samples were added to wells in triplicate and incubated at 4°C overnight. After three washes, biotinylated cytokine-specific detection antibody 1:250 was added for 1 h. After washing, the detection agent streptavidin-peroxidase was used with the substrate 3,3',5,5'-tetrametilbenzidin for 30 min. Absorbance was measured at 655 nm on a microplate reader (BioRad, Benchmark).

#### Tissue homogenates and protein measurement

Lung samples (0.2 g wet wt) from control and exposed mice were homogenized in 120 mM KCl, 30 mM phosphate buffer (pH 7.4) at 4°C (1:5). The suspension was centrifuged at 600 g for 10 min at 4°C to remove nuclei and cell debris. The pellet was discarded, and the supernatant was used as “homogenate” [31]. Protein was measured by the method of Lowry et al. [32], using bovine serum albumin as the standard.

#### Superoxide dismutase and catalase activity

Superoxide dismutase activity was determined spectrophotometrically by measuring the inhibition rate of the autocatalyzed formation of adenosine at 480 nm in a reaction medium containing 1 mM epinephrine and 50 mM glycine/NaOH (pH = 10.5) [33]. Enzymatic activity was expressed as superoxide dismutase units per milligram of protein. One unit is defined as the amount of enzyme that inhibits the rate of adenosine formation by 50%.

Catalase activity was determined by measuring the decrease in absorption at 240 nm in a reaction medium consisting of 100 mM phosphate buffer (pH 7.4) and 20 mM hydrogen peroxide [34]. Results were expressed as picomoles catalase per milligram of protein.

#### Morphological and immunocytochemical evaluation of apoptosis

Bisbenzimidazoles are cell-permeable, adenine-thymine-binding fluorescent dyes used to stain deoxyribonucleic acid (DNA). Morphological evaluation of apoptosis was performed

ex vivo on control and particle-exposed BAL cells. After incubation time, cells were washed twice with PBS, fixed in fresh acetic-methanol (1:3) for 10 min and stained with Hoechst 33258 (1 mg/ml) 5 µg/ml in PBS for 15 min. Morphological features such as pyknosis and nuclear fragmentation [35] were examined under 460 nm in a fluorescent light microscope (Axioskop Microscope, Carl Zeiss).

Immunocytochemical determination of apoptosis was carried out by the detection of activated caspase 3 and cleavage of PARP. Control and exposed BAL cells were fixed in 4% paraformaldehyde for 20 min at room temperature and permeabilized with 0.2% Triton X-100 for 7 min. Subsequently, cells were blocked with blocking buffer (PBS 0.1% Tween 20 and 5% normal serum) in a moist chamber for 2 h. Then cells were incubated either with anti-activated caspase 3 (1:500) or anti-85 kDa poly (ADP-ribose) polymerase (PARP) cleavage fragment (1:250) for 2 h. All wells were washed with PBS (two times) and PBS/0.1% Tween 20 (two times). To localize the expression of these apoptotic markers, cell smears were incubated with a secondary antibody conjugated to fluorescein isothiocyanate (1:250) for 40 min and the reaction visualized under a fluorescent light microscope (Axioskop Microscope, Carl Zeiss).

#### Statistical analysis

The results corresponding to the end-points for control and exposed animals were compared employing the analysis of variance (ANOVA) test. Statistical significance was set at

$p < 0.05$ . The number of animals and experiments for each group (control and exposed) are shown in the figure legends.

## RESULTS

### Scanning electron microscopy and EDX analysis

The morphology and spectral composition of the RR-PM is shown in Figure 2. Sediment particle size of the RR is heterogeneous, revealing the existence of a matrix, particle agglomerates, and free particles of two different sizes. First, coarse particles (PM<sub>10</sub>) and agglomerates with predominately aluminum silicates and traces of Fe and Mg were detectable by EDX (Fig. 2B). Second, small spherical fine particles (PM<sub>2.5</sub>) with not only aluminum silicates and traces of Fe and Mg but with the presence of two marked peaks—Pb and S (Fig. 2D).

As can be seen in the micrograph (Fig. 2C), the refraction of the dense granules in these fine PM<sub>2.5</sub> particles, typical of compounds with a heavy nucleus, may correspond to S, Pb, and to a lesser extent, Cr. The rest of the metals could be dispersed in the matrix associated with clay or organic matter.

### Speciation and quantification of metals in RR-PM

The presence and speciation of transition metals in the sediments of the RR were determined by BCR sequential extraction as was described in the *Materials and Methods* section. Table 1 shows corresponding values for 10 metal traces present in both the bioaccessible (first and second extractions) and the total fraction (all four sequential extractions). In Argentina, no legislation provides quality guideline values

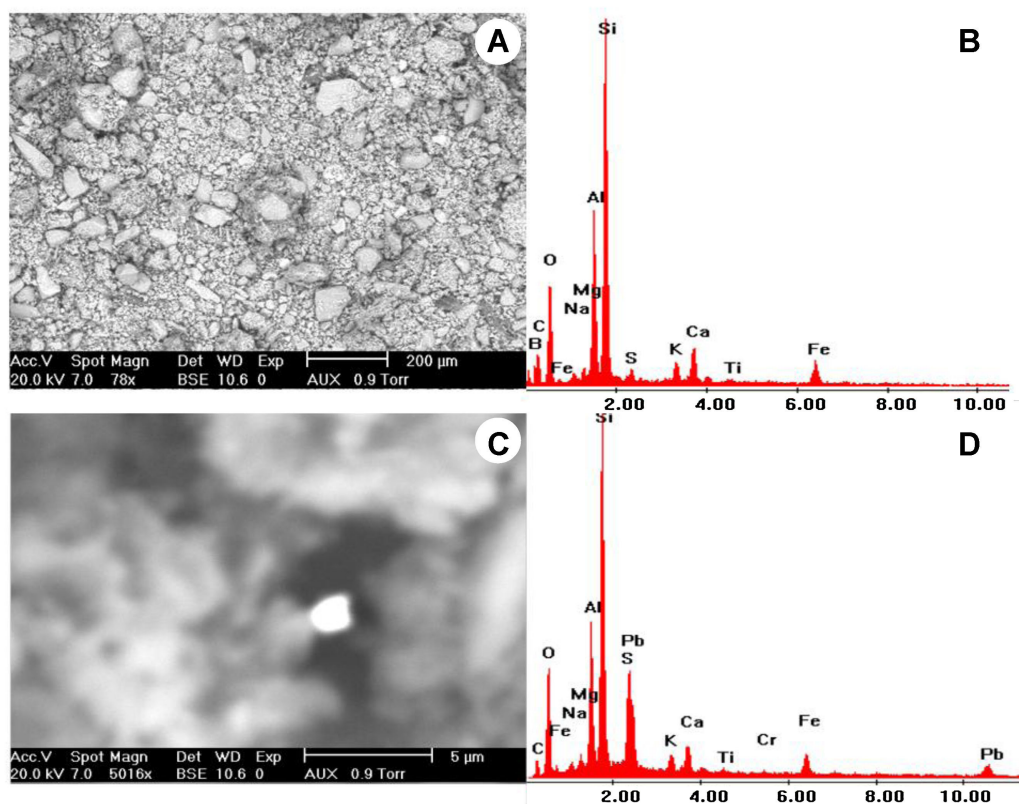


Fig. 2. (A) Scanning electron microscopy (SEM) microphotograph of sediment particles of the Reconquista River (RR-PM) showed morphological heterogeneity, found as agglomerates or associated to a matrix and fine particles. Magnification = 78 $\times$ , Scale = 200  $\mu$ m. (B) EDX Analysis of RR-PM. The characteristic elemental chemical composition evaluated by X-ray energy dispersion spectroscopy (intensity in function of energy in KeV). (C) SEM microphotograph of RR-PM showed fine particles (PM<sub>2.5</sub>). Original magnification = 5,016 $\times$ . Scale = 5  $\mu$ m. (D) EDX analysis of RR-PM fine particles. The characteristic elemental chemical composition evaluated by X-ray energy dispersion spectroscopy (intensity in function of energy in KeV). [Color figure can be seen in the online version of this article, available at [wileyonlinelibrary.com](http://wileyonlinelibrary.com)]

Table 1. BCR sequential extraction of metals present in RR-PM

	Bioavailable fraction (mg/kg sediment)	TF (mg/kg sediment)	Sediment quality guidelines (TF) (mg/kg) <sup>a</sup>
Cadmium (Cd)	3.5	70	0.8
Cobalt (Co)	10.5	29.3	20
Copper (Cu)	401	2,252.8	36
Chrome (Cr)	263.5	3,028.7	100
Nickel (Ni)	38.5	213.9	35
Lead (Pb)	325	7,065.2	85
Zinc (Zn)	> 1250	>1,250	140

<sup>a</sup>Sediment quality guidelines established for Holland [36].

BCR = Community Bureau of Reference; RR-PM = sediment particles of the Reconquista River; TF = total fraction.

for sediments. Therefore, the best approach that can be made is to compare the obtained values with the Netherlands sediment quality guideline [36]. Table 1 shows the speciation for RR-PM metal traces in which six of the elements detected (Co, Cu, Fe, Mn, Ni, and Zn) were highly bioaccessible. Bioaccessibility of heavy metals in dry sediments increases significantly compared with the wet ones because of the increased availability of oxygen that can cause a drastic change of metal speciation. Similar results on other streams in Buenos Aires were shown previously [14].

#### Total cell number, differential cell count, and lung histology

We first examined the effect of RR-PM on the TCN of BAL fluid obtained from young BALB/c mice. As shown in Figure 3A, the intranasal instillation of RR-PM provoked a marked and significant increase in TCN, both on the exposed to particles group and previously OVA-sensitized and exposed mice when compared with control nonexposed animals (exposed to particles group =  $13.7 \times 10^5 \pm 0.6 \times 10^5$ , sensitized and exposed to particles group =  $14.6 \times 10^5 \pm 0.9 \times 10^5$

vs control healthy group =  $4 \times 10^5 \pm 0.5 \times 10^5$  cells;  $p < 0.001$ ). The increase in TCN induced by RR-PM is independent of the airway condition, as no significant differences were found between exposed to particles and sensitized and exposed to particles animals. Note that OVA sensitization per se (sensitized with ovalbumin group =  $6.1 \times 10^5 \pm 1 \times 10^5$  cells) did not alter TCN. Next, we studied the BAL fluid-cell composition by analyzing the proportion of different cell types present. We evaluated the contribution of the different cell populations in the BAL fluid obtained from each animal by quantifying the percentage of polymorphonuclear cells (PMN), AM, and lymphocytes. The BAL obtained from control animals elicited a normal cell population distribution, with 85% AM and between 10 and 12% PMN. The percentage of lymphocytes remained below 3% irrespective of the treatment (Fig. 3B).

As seen in Figure 3B, RR-PM significantly augments the PMN fraction up to almost 40% in comparison with controls (exposed to particles group =  $38 \pm 2\%$  vs control healthy group =  $14 \pm 1\%$ ;  $p < 0.001$ ). Moreover, in OVA sensitized RR-PM exposed mice, the PMN fraction increased dramatically, reaching more than 60% (sensitized and exposed to particles group =  $61 \pm 4\%$  vs control healthy group =  $14 \pm 1\%$ ;  $p < 0.001$ ).

Lung histology corresponding to the lower respiratory tract of experimental groups (Fig. 4) clearly shows differences in the alveolar area. Histomorphometry (Fig. 4E) showed a marked reduction of the alveolar space in the lung for both exposed (PM) and previously OVA-sensitized and exposed mice when compared with the control group (control healthy group =  $61.8 \pm 1.8\%$  vs exposed to particles group =  $26.2 \pm 0.1\%$ , sensitized with ovalbumin group =  $37.1 \pm 0.7\%$ , sensitized and exposed to particles group =  $24.6 \pm 0.4\%$ ;  $p < 0.001$ ). This marked reduction in airspace percentage may be attributable to cell infiltration.

#### Superoxide anion generation

Because PM, depending on its chemical composition, can induce ROS, we wondered whether RR-PM was able to stimulate superoxide anion ( $O_2^-$ ) generation as one major identified ROS. Control cells were mostly nonreactive, although a few of them did exhibit scattered, insoluble dark blue formazan granules, indicating intracellular NBT reduction (Fig. 5). A known inductor of superoxide anion generation, TPA, was employed as a positive control. It is important to mention that TPA is not PM and thus serves as an unrelated positive control. The TPA-stimulated cells showed not only a larger proportion of cells responding to this compound but a higher degree of color intensity, clearly visible by light microscopy. As shown in Figure 5E, basal ROS levels were OVA-dependent because

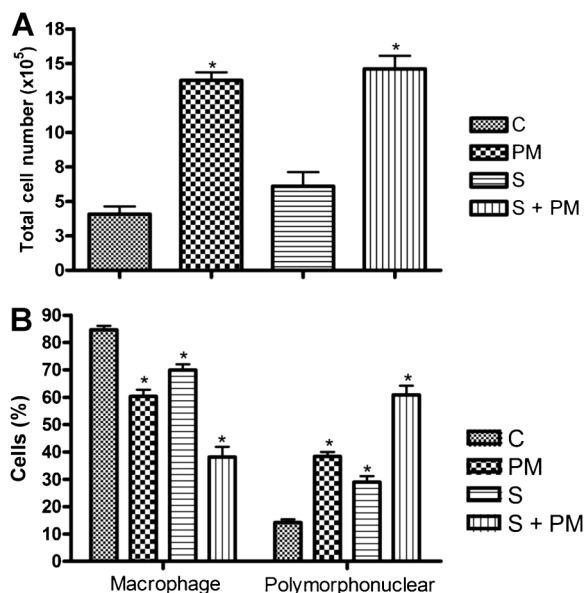


Fig. 3. (A) Histogram showing total cell numbers in the bronchoalveolar lavage (BAL) recovered from mice, and (B) histogram showing differential cell counts in the BAL recovered from mice. Controls (C), exposed to sediment particles of the Reconquista River (RR-PM), sensitized with ovalbumin (S), and both sensitized and exposed to RR-PM (S + PM). The data are mean  $\pm$  standard error,  $n = 5$  per group. \* $p < 0.001$ , analysis of variance (posttest Newman-Keuls).

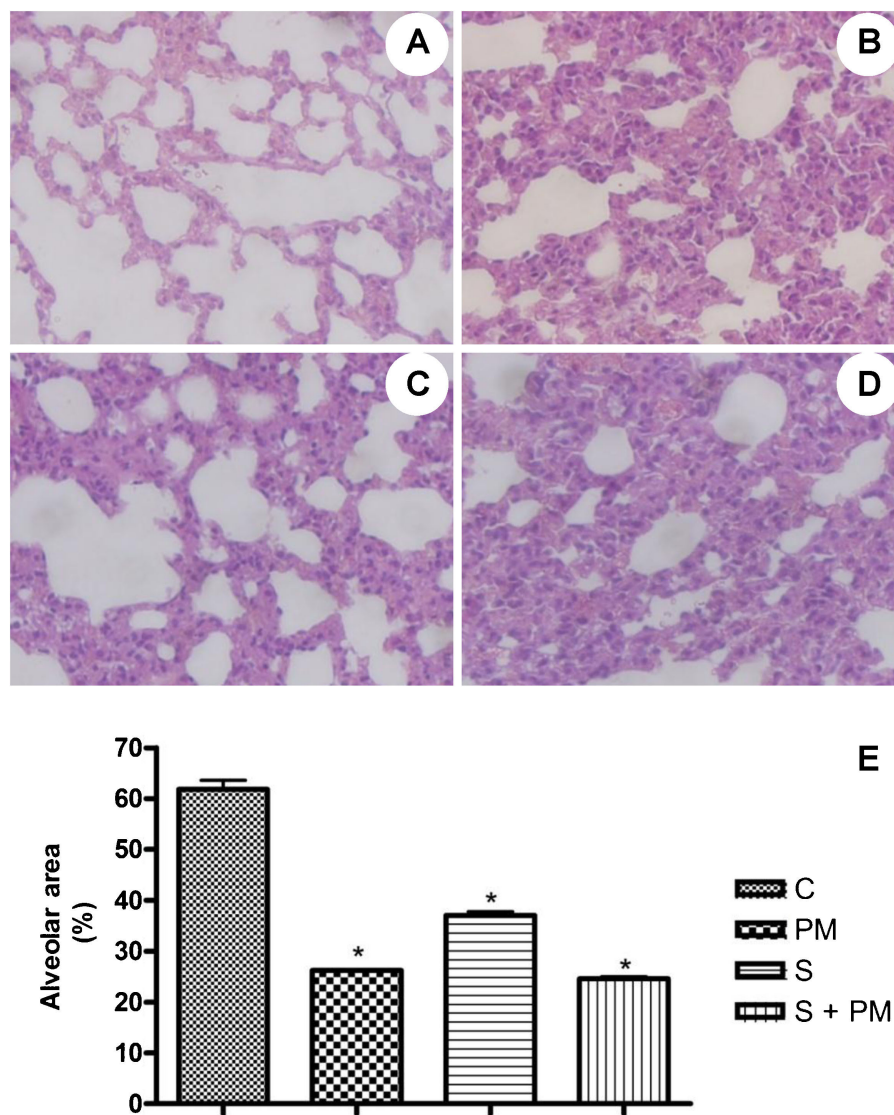


Fig. 4. Normal lung histology of the alveolar region in mice from different experimental groups, hematoxylin-eosin stain. (A) Controls, (B) exposed to sediment particles of the Reconquista River (RR-PM), (C) sensitized with ovalbumin, (D) sensitized and exposed to RR-PM. Original magnification, 100 $\times$ . (E) Histogram showing lung histomorphometry measured in microphotographs with Image Pro Plus software. Controls (C), exposed to RR-PM (PM), sensitized with ovalbumin (S) and both sensitized and exposed to RR-PM (S + PM). The data are mean  $\pm$  standard error,  $n = 5$  per group. \* $p < 0.001$ , analysis of variance (posttest Newman-Keuls). [Color figure can be seen in the online version of this article, available at [wileyonlinelibrary.com](http://www.wileyonlinelibrary.com)]

BAL recovered from sensitized animals showed a higher number of dark reactive cells (color intensity is associated with cell ability to produce  $O_2^-$ ) when compared with BAL cells from control nontreated animals. The percentage of reactive cells in control BAL was as low as  $9.8 \pm 1.1\%$ , whereas in the BAL obtained from sensitized animals was  $24.4 \pm 2.5\%$ , in agreement with what was observed by light microscopy, showing positive reaction to NBT ( $p < 0.001$ ). Moreover, a greater increase in the percentage of reactive cells was observed for both the exposed to particles and sensitized and exposed to particles groups BAL cells when compared with control healthy and sensitized with ovalbumin groups (exposed to particles group =  $38.7 \pm 1.9\%$  and sensitized and exposed to particles group =  $61.3 \pm 1.6\%$  vs control healthy group =  $9.8 \pm 1.1\%$  and sensitized with ovalbumin group =  $24.4 \pm 2.5\%$ ;  $p < 0.001$ ). Despite the differences in these four groups, TPA added to the cell suspension was able to produce a significant increase in the percentage of reactive cells, eliciting no differences among groups.

#### Evaluation of antioxidants: superoxide dismutase and catalase activities

Superoxide dismutases are a group of antioxidant enzymes that catalyze the dismutation of superoxide anion to oxygen and hydrogen peroxide. Figure 6A clearly shows that in lung homogenates from both OVA-sensitized mice, a significant decrease in superoxide dismutase activity was found with respect to their counterparts (sensitized with ovalbumin group =  $0.25 \pm 0.01$  vs control healthy group =  $0.60 \pm 0.09$  and sensitized and exposed to particles group =  $0.18 \pm 0.04$  vs exposed to particles group =  $0.61 \pm 0.02$  Usod/mg prot,  $p < 0.001$ ). Conversely, catalase, the main detoxifying system for hydrogen peroxide, was not affected (Fig. 6B).

#### Cytokine production

As described in the *Materials and Methods* section, TNF $\alpha$  and IL-6 from all four experimental animals were determined by enzyme-linked immunosorbent assay. Both proinflammatory

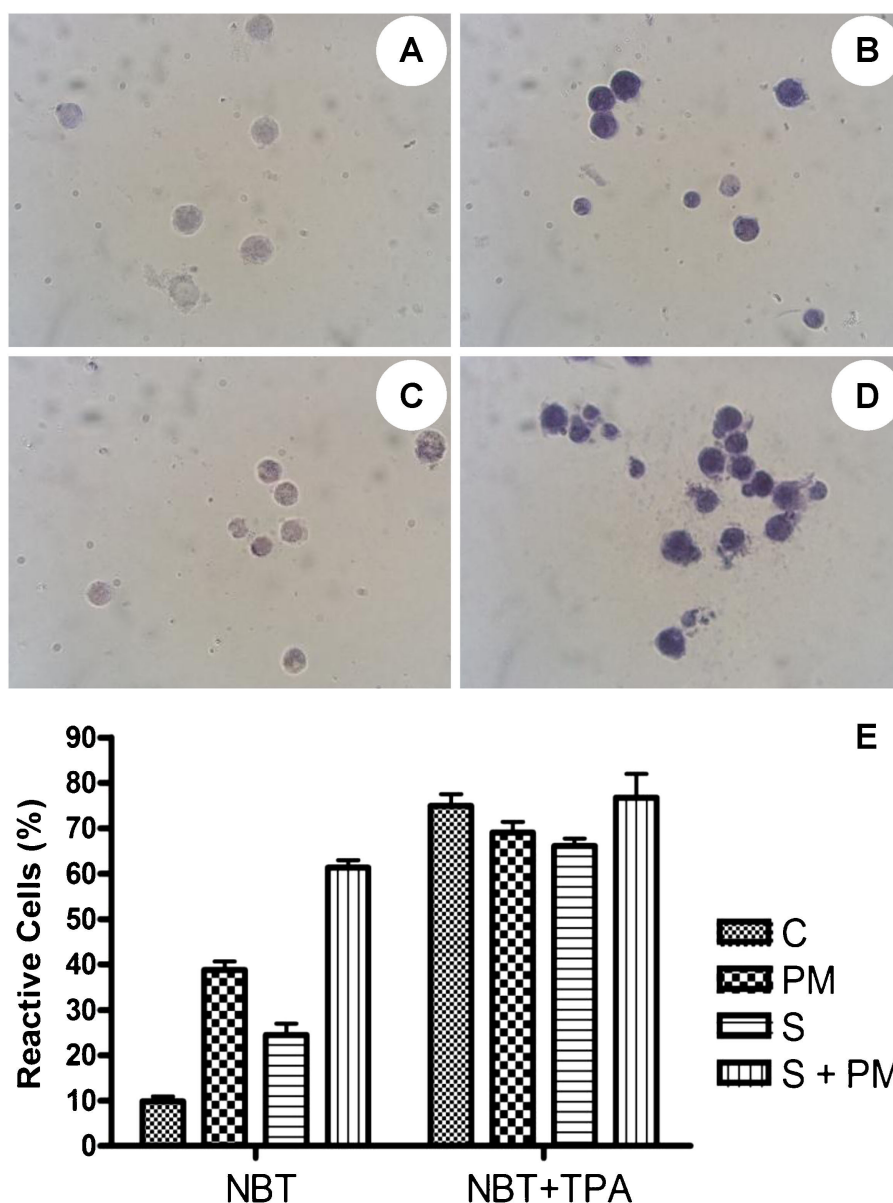


Fig. 5. Microphotograph of nitroblue tetrazolium (NBT) reaction in bronchoalveolar lavage (BAL) cells. (A) Controls, (B) exposed to sediment particles of the Reconquista River (RR-PM), (C) sensitized with ovalbumin, (D) sensitized and exposed to RR-PM. Original magnification, 400 $\times$ . (E) Histogram showing  $O_2^-$  generation measured by the reduction of NBT. Controls (C), exposed to RR-PM (PM), sensitized with ovalbumin (S) and both sensitized and exposed to RR-PM (S + PM). The data are mean  $\pm$  standard error,  $n = 5$  per group.  $^*p < 0.001$ , analysis of variance (posttest Newman-Keuls). [Color figure can be seen in the online version of this article, available at [wileyonlinelibrary.com](http://wileyonlinelibrary.com)]

cytokines provoked a similar response. The RR-PM was able to induce a significant increase in the levels of TNF $\alpha$  and IL-6 only on previously OVA-sensitized animals (Table 2).

#### Superoxide anion generation *ex vivo*

To identify whether bioaccessible metals present in the RR-PM are mainly responsible for  $O_2^-$  generation, the effects of total RR-PM, RR-PM treated with EDTA (0.1 M, pH = 5), and soluble metallic fraction (SMF) obtained after RR-PM was treated with EDTA, were evaluated on BAL cells from control mice. Superoxide anion was analyzed by means of the NBT test as described in the *Materials and Methods* section. Total RR-PM and SMF induced a significant augmentation of the percentage of reactive cells reaching similar values (RR-PM =  $44.6 \pm 1.7\%$  vs RPMI =  $10.1 \pm 1.9\%$ ; SMF =  $42.1 \pm 1.9\%$  vs EDTA =  $13.9 \pm 1.3\%$ ;  $p < 0.001$ ). The EDTA-treated PM

(RR-PM/EDTA =  $19.2 \pm 1.8\%$  vs EDTA =  $13.9 \pm 1.3\%$ ;  $p < 0.05$ ) also provoked an increase in the percentage of reactive cells, although it was much lower than that observed when cells were treated with either RR-PM or SMF. Neither RPMI-1640 nor EDTA employed as controls were able to stimulate the generation of  $O_2^-$ .

#### Morphological and immunocytochemical evaluation of apoptosis

The morphological analysis showed that most BAL cells exposed to RR-PM underwent apoptosis. The Supplemental Data shows microphotographs from control and exposed AM after the fluorescent Hoechst 33258 stain. Control nonexposed AM elicited a homogeneous chromatin nucleus. On the contrary, BAL cells exposed to RR-PM elicited characteristic apoptotic features, shrunken cytoplasm, and intense condensed chromatin in the nucleus (See Supplemental Data).

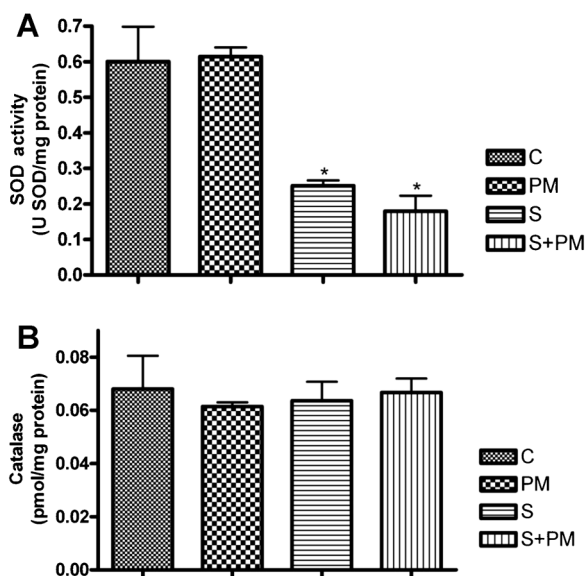


Fig. 6. (A) Superoxide dismutase activity in lung homogenates from the different experimental groups; and (B) catalase (CAT) concentration in lung homogenates from the different experimental groups. Controls (C), exposed to sediment particles of the Reconquista River (RR-PM), sensitized with ovalbumin (S), and both sensitized and exposed to RR-PM (S + PM). The data are mean  $\pm$  standard error,  $n = 5$  per group. \* $p < 0.001$ , analysis of variance (posttest Newman-Keuls).

Table 2. Proinflammatory cytokine levels measured by ELISA in BAL supernatant (TNF) or serum (IL-6) from different experimental groups

	TNF (pg/ml)	IL-6 (pg/ml)
C (Control)	54.7 $\pm$ 1.3	44.6 $\pm$ 9.3
PM (exposed to RR-PM)	116.1 $\pm$ 47.8	261.2 $\pm$ 33.1
S (sensitized with OVA)	65.6 $\pm$ 5.1	349.2 $\pm$ 105.2
S + PM (sensitized with OVA and exposed to RR-PM)	1,117.2 $\pm$ 218.4 <sup>a</sup>	1,547.2 $\pm$ 336.5 <sup>a</sup>

<sup>a</sup> $p < 0.001$ , analysis of variance (posttest Newman-Keuls).

BAL = bronchoalveolar lavage; TNF = tumor necrosis factor;

RR-PM = sediment particles of the Reconquista River; OVA = ovalbumin.

Apoptosis quantification is shown in Table 3, in which the percentage of apoptotic cells significantly increases on mice BAL cells exposed to either RR-PM or SMF. Conversely, RPMI, EDTA, and RR-PM EDTA-treated particles induced a less than 20% increase in the apoptotic index (Table 3).

The immunocytochemical study showed that RR-PM was able to induce an increase in the percentage of active-caspase 3

and PARP-positive cells, two known apoptotic markers. As clearly shown in Table 3, both biomarkers were modulated when cells were exposed to the SMF of RR-PM. These two fractions induce significant differences in the apoptotic index ( $p < 0.001$ ) when compared with EDTA-treated RR-PM or control RPMI-1640 and EDTA (Table 3). Microphotographs from control cells treated for caspase 3 or PARP, respectively, are shown in the Supplemental Data. To better visualize the nuclei, the insets in those figures show the Hoechst reaction. Soluble metallic fraction provokes a rise in the caspase 3 and PARP biomarkers in BAL cells, respectively.

## DISCUSSION

The RR has been subjected to contaminating materials capable of initiating the impairment of the water quality and thus polluting its sediments. The sediments of rivers and streams act as sinks for toxic substances, and thus the persistent pollutants such as heavy metals often accumulate in them [37]. Herein, we showed that the mean value concentrations from certain associated heavy metals of the surface sediment—such as Co, Cu, Fe, Mn, Ni, and Zn—in RR-PM are much higher than those found in streams not subject to contamination [38] and to the Netherlands sediment-quality guidelines. These high values can be adduced to anthropogenic (industrial and domestic) activities going on along the RR basin. In agreement with Adeniyi et al. [39] and Aderinola et al. [40], the present study confirms that sediments are important hosts to heavy metals. In addition, changes in the redox conditions of the system, such as those generated by drying, often produce increases in the bioavailability of heavy metals accumulated in the sediments [14,37]. Heavy metals such as Cr, Ni, Pb, Cd, and As are toxic to all levels of biota, including mammals; Cr (VI), Ni, and Cd are carcinogenic, As and Cd are teratogenic, and Pb can provoke neurological impairment and malfunctioning of the central nervous system. Sediments adsorbed with metals always show more drastic and deleterious effects [41,42].

The present study revealed that dry sediment particles from the shore of RR included heavy metals in their chemical composition and had mean aerodynamic diameters below 2.5  $\mu\text{m}$  ( $\text{PM}_{2.5}$ ), allowing them to enter into the respiratory system and reach the alveolar region in the lungs. We showed that the adverse effects observed on RR-PM exposed animals in vivo on their respiratory tract and ex vivo on the BAL fluid were largely dependent on the heavy metal content. Because of the oxidation of sulfides and of the organic matter, the sediments are changed during dry seasons, modifying the heavy metals speciation to a more bioaccessible form that increases the

Table 3. Morphological (Hoechst) and immunocytochemical (PARP and Caspase 3) evaluation of apoptosis performed on BAL cells

Treatment	Percentage of apoptotic cells (%)		
	Hoechst	Caspase 3	PARP
RPMI (Control group)	11.6 $\pm$ 3.7	10.4 $\pm$ 4.3	9.6 $\pm$ 3.4
EDTA (Cells exposed to EDTA)	16.9 $\pm$ 3.9	18.4 $\pm$ 5.6	17.5 $\pm$ 4.3
RR-PM/EDTA (Cells exposed to treated RR-PM)	14.3 $\pm$ 2.1	24.2 $\pm$ 3.3	21.2 $\pm$ 4.5
RR-PM (Cells exposed to RR-PM)	50.1 $\pm$ 1.9 <sup>a</sup>	66.8 $\pm$ 6.1 <sup>a</sup>	69.4 $\pm$ 2.9 <sup>a</sup>
SMF (Cells exposed to soluble metallic fraction)	49.2 $\pm$ 3.8 <sup>b</sup>	74.3 $\pm$ 7.8 <sup>b</sup>	75.9 $\pm$ 5.6 <sup>b</sup>

<sup>a</sup> $p < 0.001$  versus RPMI, analysis of variance (posttest Newman-Keuls).

<sup>b</sup> $p < 0.001$  versus EDTA, analysis of variance (posttest Newman-Keuls).

BAL = bronchoalveolar lavage; RPMI = RPMI-1640 medium; EDTA = ethylenediaminetetra-acetic acid; RR-PM = sediment particles of the Reconquista River; SMF = soluble metal fraction.



adverse effects of the particulate matter. Exposure to RR-PM increased TCN and altered the composition of the cell population normally present in the BAL. The augment in TCN was the result of increases in the PMN population, which in turn and in agreement with Martin et al. [27] may result in a reduction of the alveolar space. In agreement with Antonini et al. [43], the rise in the PMN fraction could be reflecting the chemical composition of the particle. These researchers reported that residual oil fly ash, a surrogate of ambient pollution with an elevated metal content, mainly vanadium, increased the BAL PMN fraction [43,44].

In this context, from our *in vivo* experiments we believe that inhaled PM<sub>2.5</sub> from the RR sediments undergo phagocytosis by alveolar macrophages, which in response release mediators such as superoxide anion (O<sub>2</sub><sup>-</sup>), a major ROS, and the pro-inflammatory cytokines TNF $\alpha$  and IL-6. The mechanism of oxidant activation triggered by a variety of PM is cell specific and depends on the nature of the pollutant [45]. In any case, severe increases in ROS can induce cell death [46,47]. As was clearly shown in our *ex vivo* experiments done on BAL cells, RR-PM and the SMF were able to induce O<sub>2</sub><sup>-</sup> and apoptosis to a similar extent when compared with controls. On the contrary, when RR-PM was depleted from the metallic fraction, almost no changes were observed in comparison with nonexposed cells. Our findings were consistent when apoptosis was determined morphologically or immunocytochemically using specific antibodies against caspase 3 and its substrate PARP. In this regard, our data reinforce the concept that oxidative stress and increased apoptosis play a role in particle-mediated lung injury.

Not only does strong epidemiological evidence exist of a relationship between particle pollution and exacerbation of asthma, but recent studies, particularly in urban areas, have suggested a role for pollutants in the development of both asthma and chronic obstructive pulmonary disease [48,49]. Accordingly, we found that the RR-PM behavior as described for normal animals held true also for OVA-exposed animals, even more; we found exacerbation of the biological response regarding O<sub>2</sub><sup>-</sup> generation and secretion of both pro-inflammatory cytokines TNF $\alpha$  and IL-6. Even though animals from the sensitized with ovalbumin group *per se* have shown increased TCN, PMN, and ROS generations, RR-PM exposure was able to further enhance this biological response. Thus, our results show that exposure to RR-PM enhances immune responsiveness and the severity of pulmonary inflammation in both normal and OVA-exposed mice.

We propose that the adverse effect observed both *in vivo* and *ex vivo* is initiated by ROS, which fires an imbalance in the redox metabolism, which in turn alters the proinflammatory cytokine profile and induces PMN recruitment.

## CONCLUSION

We found that exposure to RR-PM resulted in increased pulmonary inflammation and occurrence of apoptosis in mice. These events correlated with the presence of bioaccessible heavy metals in the particles and caused an increase in various oxidative stress markers, suggesting that oxidative stress may, in part, be responsible for these adverse effects. We conclude that RR-PM exposure enhances immune responses to allergens and thus exacerbates immune-mediated lung diseases.

*Acknowledgement*—All of the authors have no conflict of interest to declare. The present study was partially supported by Grants A097 and A105 from the National University of General San Martín and PIP 11220090100079, CONICET, 2010-2012. The experiments reported here were conducted

according to principles set forth in the Guide for the Care and Use of Laboratory Animals (NIH, 1985), the EC Directive 86/609/EEC, and the committee ad hoc of the School of Science and Technology, National University of General San Martín.

## SUPPLEMENTAL DATA

Microphotographs of BAL cells stained with Hoechst 33258: (A) control and (B) RR-PM group and immunodetection of both apoptotic biomarkers (C and E) caspase 3 and (D and F) PARP. (C–D) control cells and (E–F) soluble metallic fraction (SMF) exposed cells. Insets show DAPI stain. Original magnification 1,000 $\times$ . (37 KB PDF).

## REFERENCES

- Bates DV, Sizto R. 1987. Air pollution and hospital admissions in Southern Ontario: The acid summer haze effect. *Environ Res* 43: 317–331.
- Bates MN, Garrett N, Graham B, Read D. 1998. Cancer incidence, morbidity and geothermal air pollution in Rotorua, New Zealand. *Int J Epidemiol* 27:10–14.
- Dockery DW, Pope CA 3rd, Xu X, Spengler JD, Ware JH, Fay ME, Ferris BG Jr, Speizer FE. 1993. An association between air pollution and mortality in six U.S. cities. *N Engl J Med* 329:1753–1759.
- Black H. 1994. The price of progress: Environmental health in Latin America. *Environ Health Perspect* 102:1024–1028.
- Castañé PM, Rovedatti MG, Topalián ML, Salibián A. 2006. Spatial and temporal trends of physicochemical parameters in the water of the Reconquista River (Buenos Aires, Argentina). *Environ Monit Assess* 117:135–144.
- Herkovits J, Perez-Coll CS, Herkovits FD. 1996. Ecotoxicity in the Reconquista River, province of Buenos Aires, Argentina: A preliminary study. *Environ Health Perspect* 104:186–189.
- Topalián ML, Castañé PM, Rovedatti MG, Salibián A. 1999. Principal component analysis of dissolved heavy metals in water of the Reconquista River (Buenos Aires, Argentina). *Bull Environ Contam Toxicol* 63:484–490.
- Lee S, Moon JW, Moon HS. 2003. Heavy metals in the bed and suspended sediments of Anyang River, Korea: Implications for water quality. *Environ Geochem Health* 25:433–452.
- Sin SN, Chua H, Lo W, Ng LM. 2001. Assessment of heavy metal cations in sediments of Shing Mun River, Hong Kong. *Environ Int* 26:297–301.
- Kishe MA, Machwa JF. 2003. Distribution of heavy metals in sediments of Mwanza Gulf of Lake Victoria, Tanzania. *Environ Int* 28:619–625.
- Ahmed F, Hawa Bibi M, Hussain M, Hiroaki I. 2005. Present environment and historic changes from the record of lake sediments, Dhaka City, Bangladesh. *Environ Geol* 48:25–36.
- Balkis N, Aksu A, Okus E, Apak R. 2010. Heavy metal concentrations in water, suspended matter, and sediment from Gökova Bay, Turkey. *Environ Monit Assess* 167:359–370.
- Tack FM, Lapauw F, Verloo MG. 1997. Determination and fractionation of sulphur in a contaminated dredged sediment. *Talanta* 44:2185–2192.
- Di Nanno MP, Curutchet G, Ratto S. 2007. Anaerobic sediment potential acidification and metal release risk assessment by chemical characterization and batch re-suspension experiences. *J Soil Sediment* 7:187–194.
- Löser C, Zehnsdorf A, Voigt K, Seidel H. 2004. Physicochemical conditioning of dredged heavy metal-polluted sediment in suspension. *Eng Life Sci* 4:258–265.
- Schwartz J, Dockery DW. 1992. Increased mortality in Philadelphia associated with daily air pollution concentrations. *Am Rev Respir Dis* 145:600–604.
- Thurston GD, Ito K, Kinney PL, Lippmann M. 1992. A multiyear study of air pollution and respiratory hospital admissions in three New York State metropolitan areas: Results for 1988 and 1989 summers. *J Expos Anal Environ Epidemiol* 2:429–450.
- Pope CA III, Thun MJ, Namboodiri MM, Dockery DW, Evans JS, Speizer FE, Heath CW Jr. 1995. Particulate air pollution as a predictor of mortality in a prospective study of U.S. adults. *Am J Respir Crit Care Med* 151:669–674.
- Ure AM, Quevauviller PH, Muntauc H, Griepink B. 1993. Speciation of heavy metals in soils and sediments: An account of the improvement and harmonization of extraction techniques undertaken under the auspices of the BCR of the Commission of the European Communities. *Int J Environ Anal Chem* 51:135–151.

20. Marbán L, Giuffré L, Ratto S, Agostini A. 1999. Contaminación con metales pesados en un suelo de la cuenca del río Reconquista. *Ecología Austral* 9:15–19.
21. Kartal S, Aydn Z, Tokaloglu S. 2006. Fractionation of metals in street sediment samples by using the BCR sequential extraction procedure and multivariate statistical elucidation of the data. *J Hazard Mater* 132: 80–89.
22. Tokaloglu S, Kartal S. 2005. Comparison of metal fractionation results obtained from single and BCR sequential extractions. *Bull Environ Contam Toxicol* 75:180–188.
23. Goldsmith CA, Hamada K, Ning Y, Qin G, Catalano P, Krishna Murthy GG, Lawrence J, Kobzik L. 1999. Effects of environmental aerosols on airway hyperresponsiveness in a murine model of asthma. *Inhal Toxicol* 11:981–998.
24. Fenoy I, Giovannoni M, Batalla E. 2009. *Toxoplasma gondii* infection blocks the development of allergic airway inflammation in BALB/c mice. *Br Soc Immunol Clin Exp Immunol* 155:275–284.
25. Leong BK, Coombs JK, Sabaitis CP, Rop DA, Aaron CS. 1998. Quantitative morphometric analysis of pulmonary deposition of aerosol particles inhaled via intratracheal nebulization, intratracheal instillation or nose-only inhalation in rats. *J Appl Toxicol* 18:149–160.
26. Southam DS, Dolovich M, O'Byrne PM, Inman MD. 2002. Distribution of intranasal instillations in mice: Effects of volume, time, body position, and anesthesia. *Am J Physiol Lung Cell Mol Physiol* 282:833–839.
27. Martin S, Dawidowski L, Mandalunis P, Cereceda-Balic F, Tasat DR. 2007. Characterization and biological effect of Buenos Aires urban air particles on mice lungs. *Environ Res* 105:340–349.
28. Tasat DR, De Rey BM. 1987. Cytotoxic effect of uranium dioxide on rat alveolar macrophages. *Environ Res* 44:71–81.
29. Segal AW. 1974. Nitroblue-tetrazolium tests. *Lancet* 2:1248–1252.
30. Molinari BL, Tasat DR, Fernandez ML, Duran HA, Curiale J, Stoliar A, Cabrini RL. 2000. Automated image analysis for monitoring oxidative burst in macrophages. *Anal Quant Cytol Histol* 22:423–427.
31. Llesuy S, Evelson P, González-Flecha B, Peralta J, Carreras MC, Poderoso JJ, Boveris A. 1994. Oxidative stress in muscle and liver of rats with septic syndrome. *Free Radic Biol Med* 16:445–451.
32. Lowry OH, Rosebrough NJ, Farr AL, Randall RJ. 1951. Protein measurement with the Folin phenol reagent. *J Biol Chem* 193:265–275.
33. Misra HP, Fridovich I. 1972. The generation of superoxide radical during the autoxidation of hemoglobin. *J Biol Chem* 247:6960–6962.
34. Chance B. 1954. The assay of catalases and peroxidases. *Methods Biochem Anal* 1:357–424.
35. Singhal PC, Sharma P, Kapasi AA, Reddy K, Franki N, Gibbons N. 1998. Morphine enhances macrophage apoptosis. *J Immunol* 160:1886–1893.
36. Ministry of Housing, Spatial Planning, and the Environment. 2006. Intervention values and target values—soil quality standards. The Hague, The Netherlands.
37. Lors C, Tiffreau C, Laboudigue A. 2004. Effects of bacterial activities on the release of heavy metals from contaminated dredged sediments. *Chemosphere* 56:619–630.
38. Ronco AE, Camilión MC, Manassero MJ. 2001. Geochemistry of heavy metals in bottom sediments from streams of the western coast of the Río de la Plata estuary, Argentina. *Environ Geochem Health* 23: 89–103.
39. Adeniyi AA, Yusuf KA, Okedeyi OO. 2008. Assessment of the exposure of two fish species to metals pollution in the Ogun river catchments, Ketu, Lagos, Nigeria. *Environ Monit Assess* 137:451–458.
40. Aderinola OJ, Clarke EO, Olarinmoye OM, Kusemiju V, Anatekhai MA. 2009. Heavy metals in surface water, sediments, fish and periwinkles of Lagos Lagoon. *American-Eurasian J Agric Environ Sci* 5:609–617.
41. Markus J, McBratney AB. 2001. A review of the contamination of soil with lead II. Spatial distribution and risk assessment of soil lead. *Environ Int* 27:399–411.
42. Nadal M, Schuhmacher M, Domingo JL. 2004. Metal pollution of soils and vegetation in an area with petrochemical industry. *Sci Total Environ* 321:59–69.
43. Antonini JM, Taylor MD, Leonard SS, Lawryk NJ, Shi X, Clarke RW, Roberts JR. 2004. Metal composition and solubility determine lung toxicity induced by residual oil fly ash collected from different sites within a power plant. *Mol Cell Biochem* 255:257–265.
44. Costa DL, Lehmann JR, Jaskot R, Winsett DW, Richards J, Ledbetter AD, Dreher KL. 2006. Comparative pulmonary toxicological assessment of oil combustion particles following inhalation or instillation exposure. *Toxicol Sci* 91:237–246.
45. Becker S, Dailey LA, Soukup JM, Grambow SC, Devlin RB, Huang YC. 2005. Seasonal variations in air pollution particle-induced inflammatory mediator release and oxidative stress. *Environ Health Perspect* 113: 1032–1038.
46. Biswas SK, Rahman I. 2008. Environmental toxicity, redox signaling and lung inflammation: the role of glutathione. *Mol Aspects Med* 30: 60–76.
47. Trachootham D, Lu W, Ogasawara MA, Nilsa RD, Huang P. 2008. Redox regulation of cell survival. *Antioxid Redox Signal* 10:1343–1374.
48. Gilmour MI. 1995. Interaction of air pollutants and pulmonary allergic responses in experimental animals. *Toxicology* 105:335–342.
49. Kelly FJ, Fussell JC. 2011. Air pollution and airway disease. *Clin Exp Allergy* 41:1059–1071.